Study on the H/V Spectral Ratio Characteristics from SEIS Observation

Wanbo Xiao and Yanbin Wang
May 4, 2020
(wbxiao@pku.edu.cn)

CONTENTS

Background: Studies on the H/V spectral ratio (HVSR)

On Earth:

- Microseisms caused by ocean waves produce HVSR peak at 0.15-0.2 Hz (Tanimoto et al., 2006).
- Wind increases the amplitude of all components of the microtremor, but does not affect HVSR. (Mucciarelli et al., 2005).

On Moon:

- The peak frequency of HVSR at Apollo seismic stations is 0.7-1.7 Hz (Nakamura et al., 1975).

On Mars:

- The background noise recorded by the Viking lander 2 is highly related to the local wind speed (Nakamura et al., 1979).
- At the InSight landing site, the resonance frequency of the regolith is 6-9 Hz while those of the LVL, lander mode and solar panels are above 10 Hz, and these resonances can be distinguished by their damping ratios (Knapmeyer-Endrun, 2018).

Martian observation environment:

- severe diurnal temperature variation (~80 ℃) and continuous strong wind (over 5 m/s at daytime and below 3 m/s at nighttime averagely)

Any influence on HVSR measurement?

Methods: H/V spectral ratio (HVSR) method

ratio of horizontal to vertical Fourier amplitude spectrum in each sliding time window (Nakamura, 1989)

Source of HVSR peak

- may be related to S-wave resonance, Rayleigh wave ellipticity or Love wave air phase

Validity of HVSR peak

- Alberto (2006) proposed the random decrement method to calculate the damping ratio of seismic records.
- widely used to verify the validity of H/V peak (Dunand et al., 2002; Ebrahim, 2005; Guillier et al., 2007)

Parameters in this study

- length of sliding window: 164 s
- sample interval of seismic records: 0.01 s
- number of FFT point: 8192
- number of taper point: 10
- smooth factor: b=50

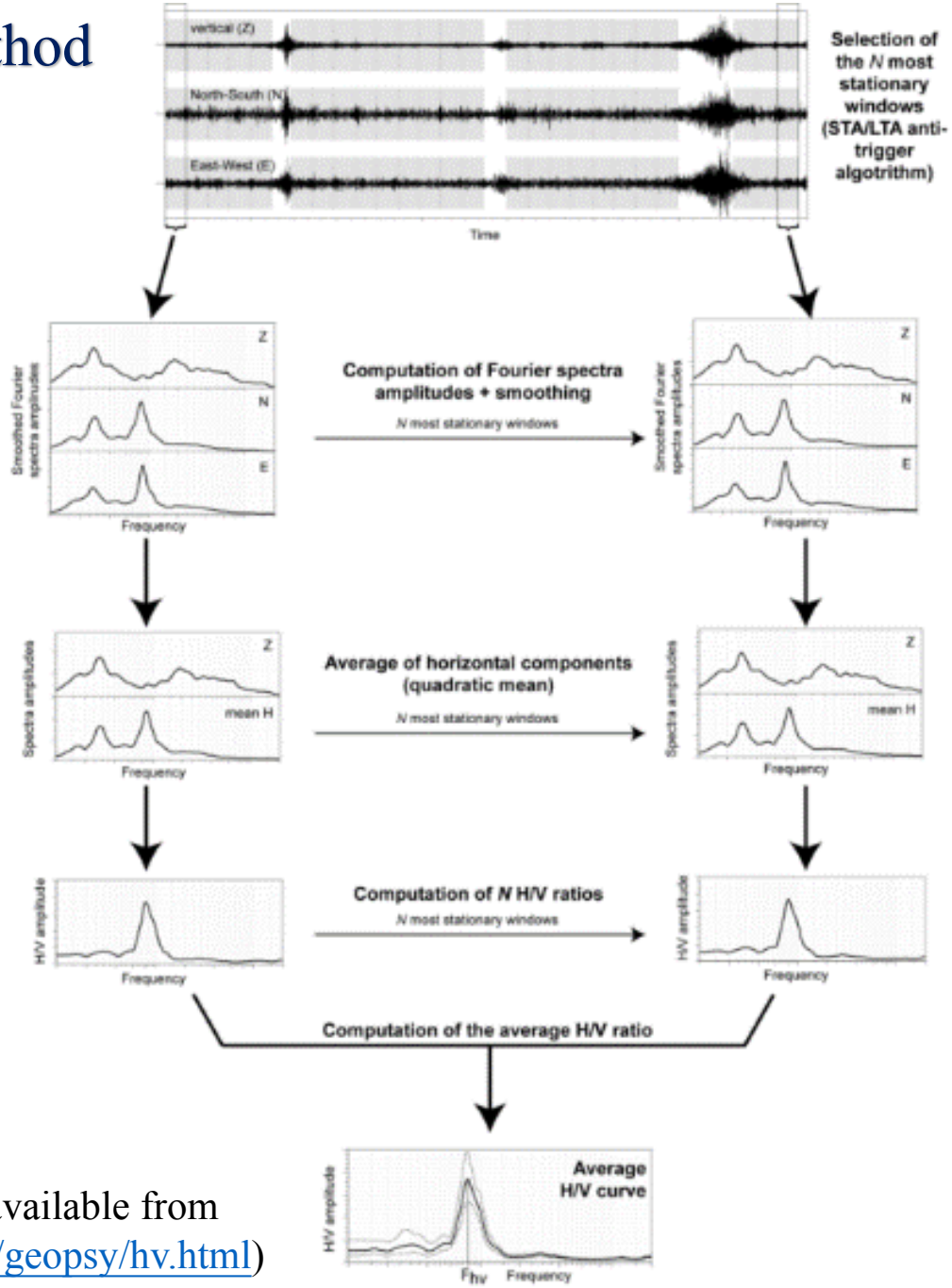

(Criteria for reliable H/V curve, available from http://geopsy.org/documentation/geopsy/hv.html)

Methods: Random decrement method (RDM)

Procedure to calculate the damping ratio at 12 Hz

- Filter data (5-20 Hz)
- Set crossing level (**green line** in the first panel)
- Find starting points (**red cross marks** in the first panel)
- Select the data segments with a fixed length (1 s) from the starting points, and average these data segments to get the **random decrement signal** (the second panel)
- Filter the random decrement signal (11-13 Hz)
- **Fit** the damping curve (the third panel)
  - **black solid line**: damping curve to be fitted
  - **red solid line**: curve that only fits the peak amplitudes by least square method
  - **red dotted line**: curve that fits the damping curve by least square method
  - **R**: the correlation coefficient of least square method
  - **DR**: damping ratio by least square method (DR of a natural source is above 5%.)

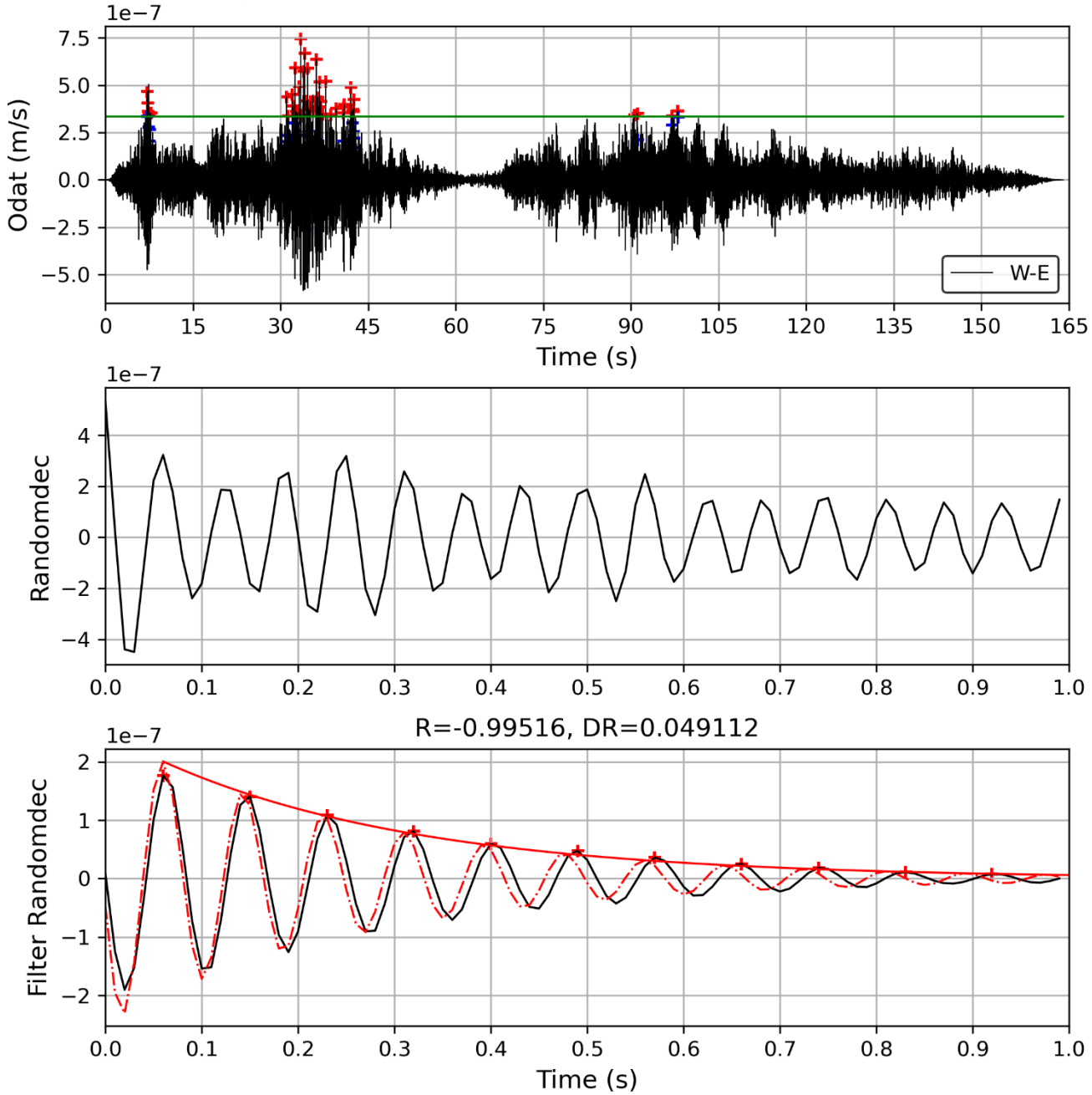

Results: Comparison between VBB and SP data

HVSR results

Both VBB and SP data have a sample rate of 100 ps.

VBB (Very Broad Band)

peak frequency: 24.5 Hz
mean peak value: 8.5
proportion with obvious H/V peak:
602/791 = 76.1%

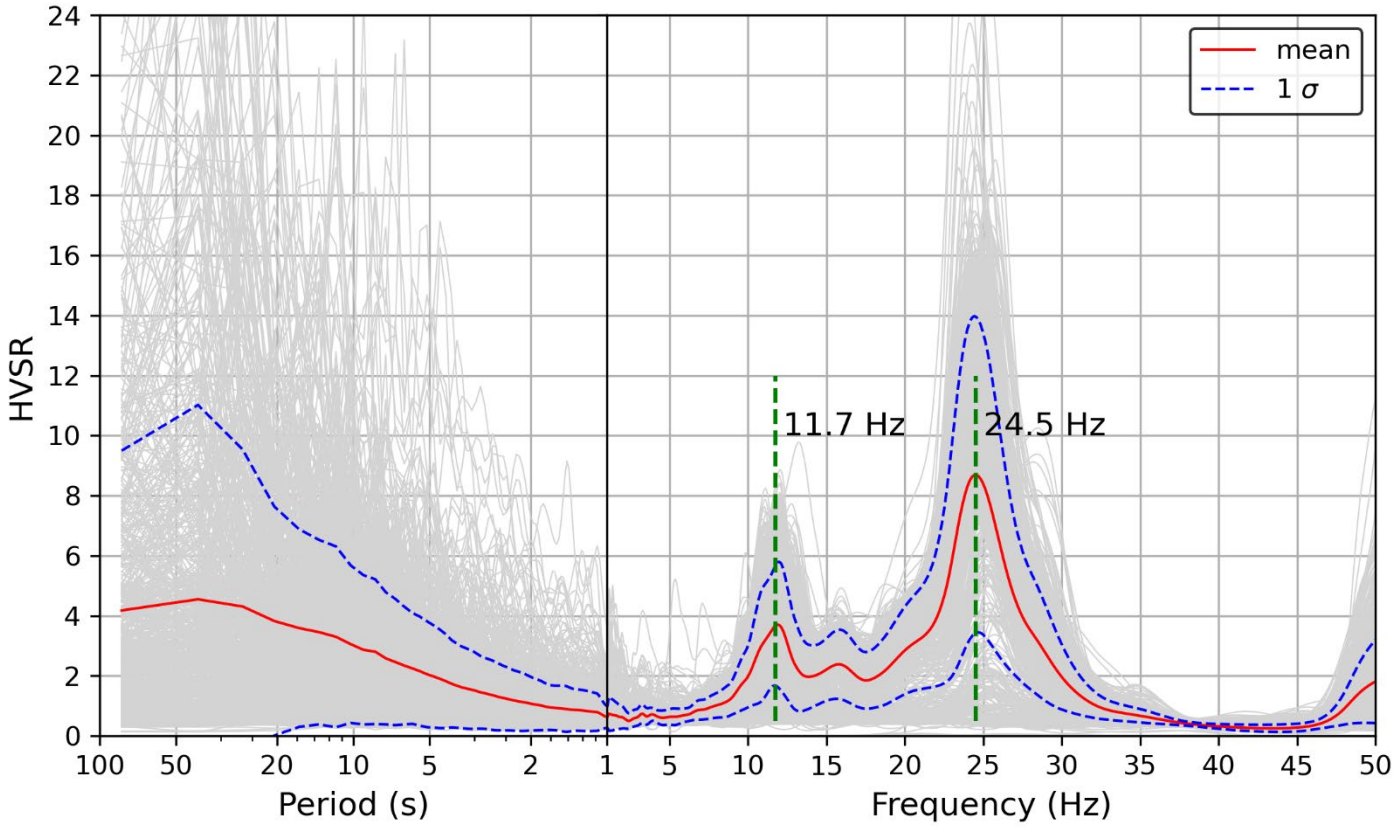

The seismic dataset used here is from 2019-02-10 to 2019-03-09 (UTC time)

Results: Comparison between VBB and SP data

HVSR results

Both VBB and SP data have a sample rate of 100 ps.

VBB (Very Broad Band)
peak frequency: 24.5 Hz
mean peak value: 8.5
proportion with obvious H/V peak:
602/791 = 76.1%

SP (Short Period)
peak frequency: 11.7 Hz
mean peak value: 6.5
proportion with obvious H/V peak:
747/791 = 94.4%

The seismic dataset used here is from 2019-02-10 to 2019-03-09 (UTC time)

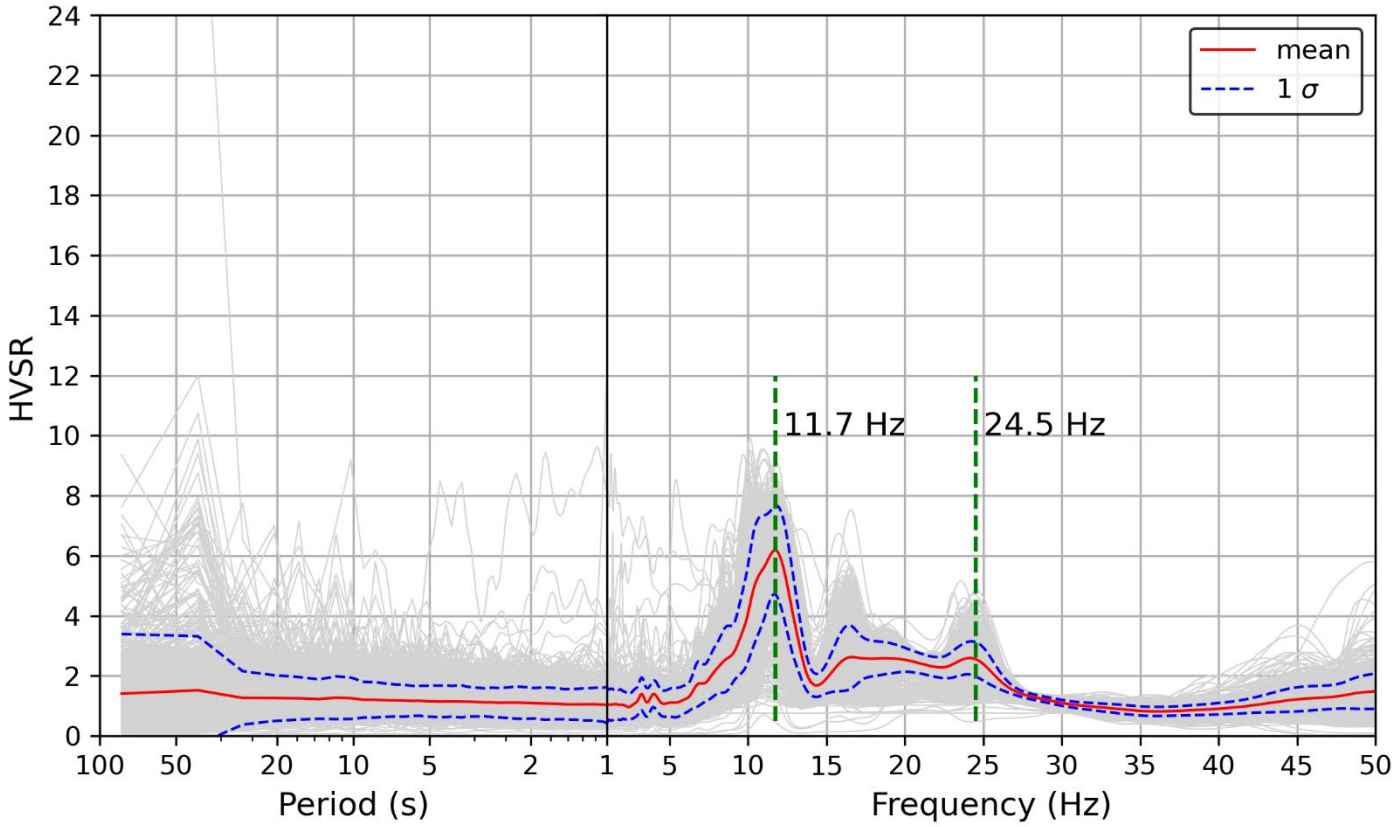

Results: Comparison between VBB and SP data

Fourier amplitude spectrums (FAS)

VBB and SP data are projected to the N-S, W-E, and Z axes.

Similarity:

- large amplitude in low (<0.1 Hz) and high (>10 Hz) frequency parts
- same resonance frequency in horizontal components

Difference:

- no obvious peak in the FAS of VBB-Z in high frequency part (20-30 Hz)
- high H/V value of VBB data at 24.5 Hz

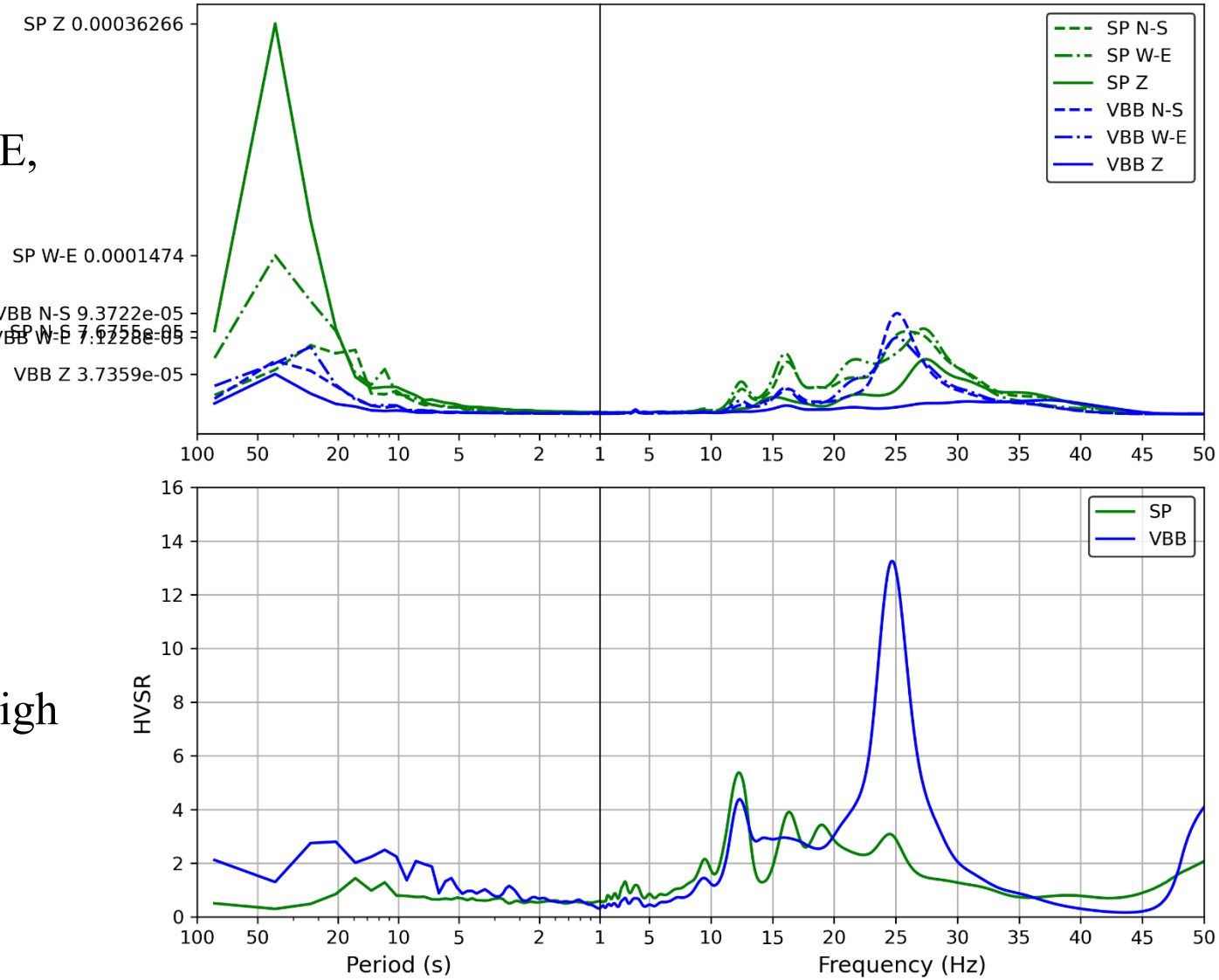

data time span: 2019.041.214154-2019.041.214438 (UTC)

Results: Comparison between VBB and SP data

Waveforms

VBB and SP data are projected to the N-S, W-E, and Z axes.

- similar waveforms in the horizontal components
- VBB-Z has smaller amplitude than SP-Z.

There is correlation between the three **original** components of VBB data in low frequency part (Lognonné et al., 2020)

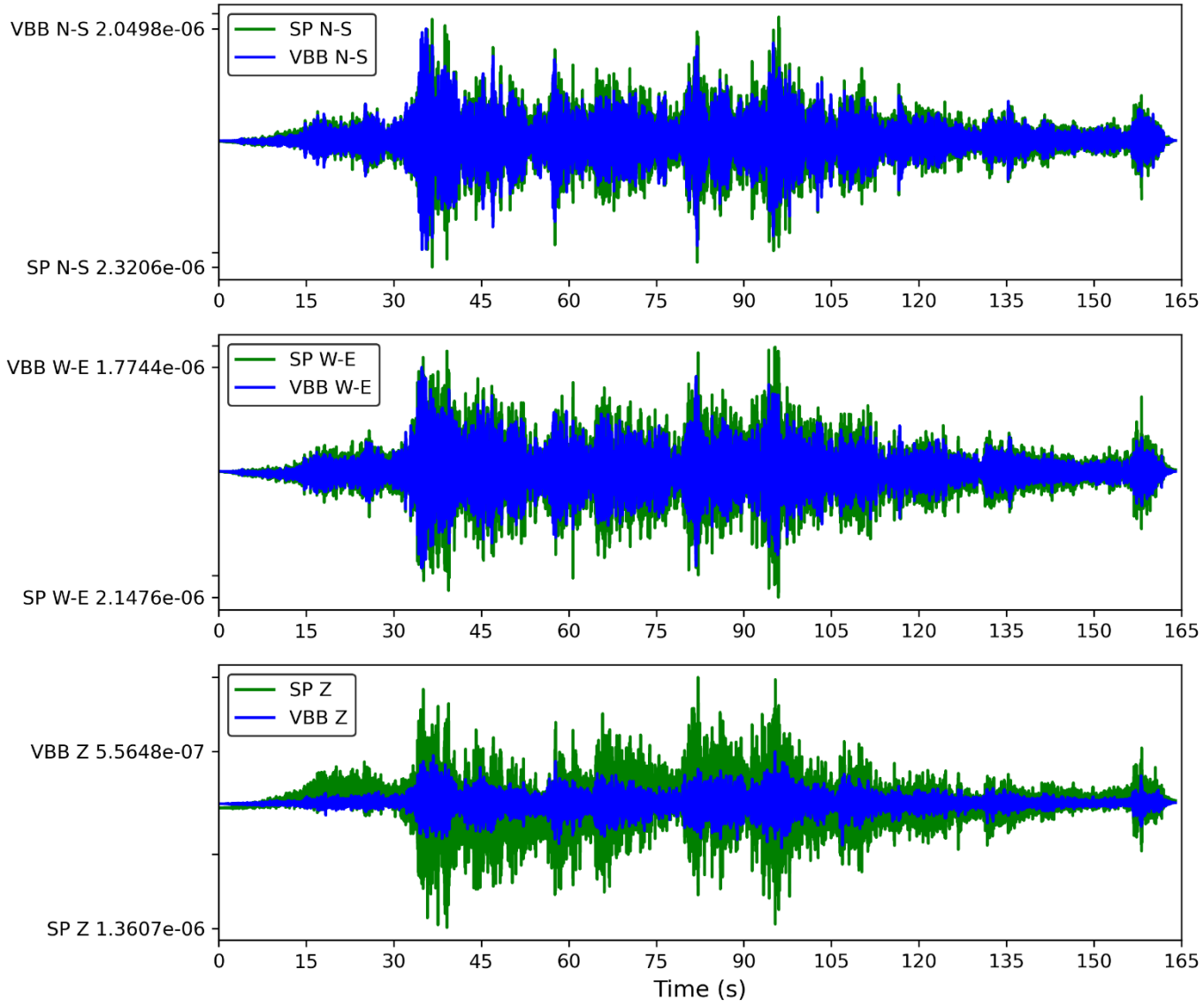

data time span: 2019.041.214154-2019.041.214438 (UTC)

Results: Comparison between SP data on lander deck and ground

HVSR results

SP data on lander deck (before UTC-2019.02.10)

- peak frequency: 11.7 Hz
- mean peak value: 8.0
- no obvious peak above 15 Hz
- unstable below 1.0 Hz

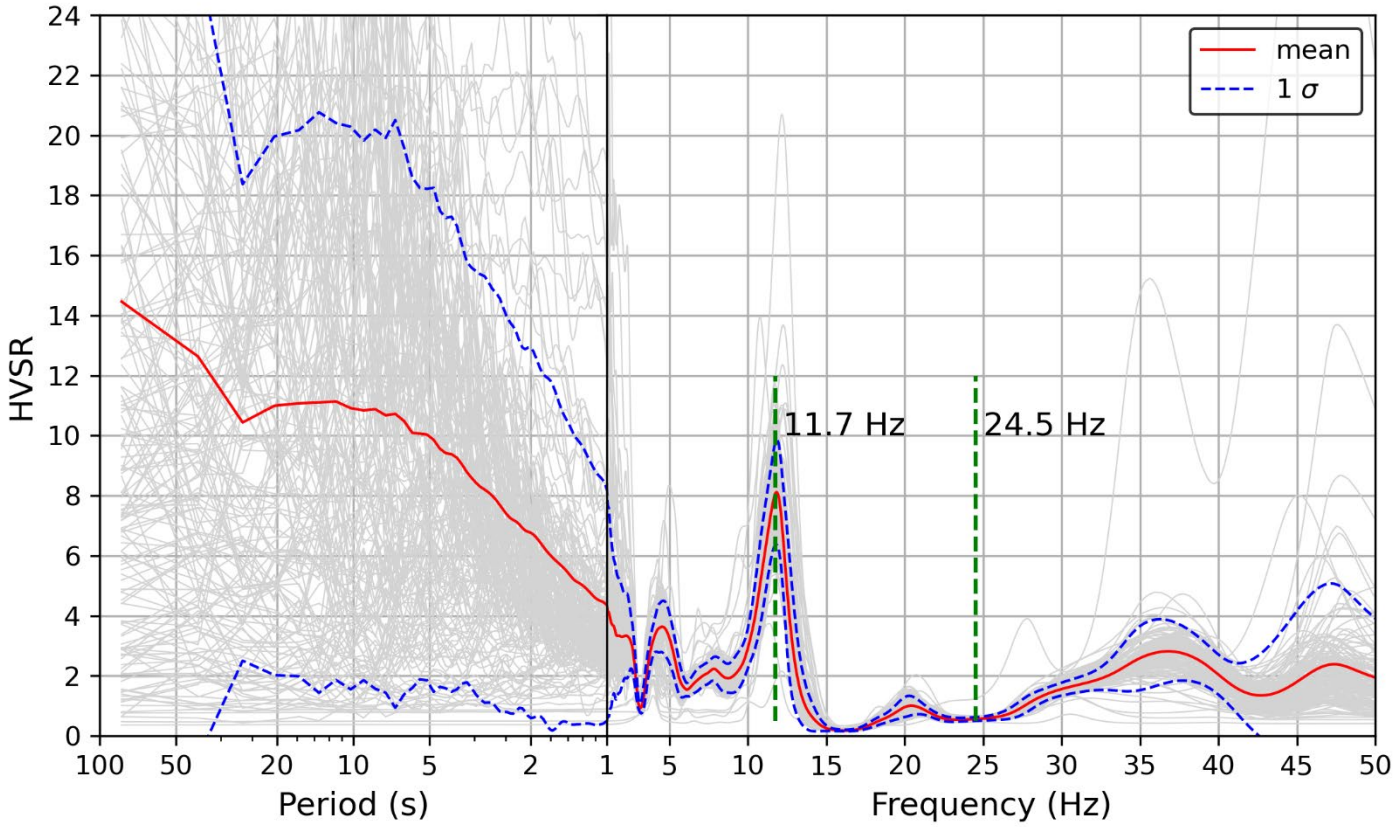

The seismic dataset used here is from 2018-12-07 to 2018-12-11 (UTC time)

Results: Comparison between SP data on lander deck and ground

SP data on lander deck

Fourier amplitude spectrums

- **sharp** peaks in each component
- several peaks in the frequency range of **2-12 Hz** in the horizontal components
- high peak at **16 Hz** in the vertical component

Waveforms

- large amplitude in all components
- **obvious tilt** in the horizontal components

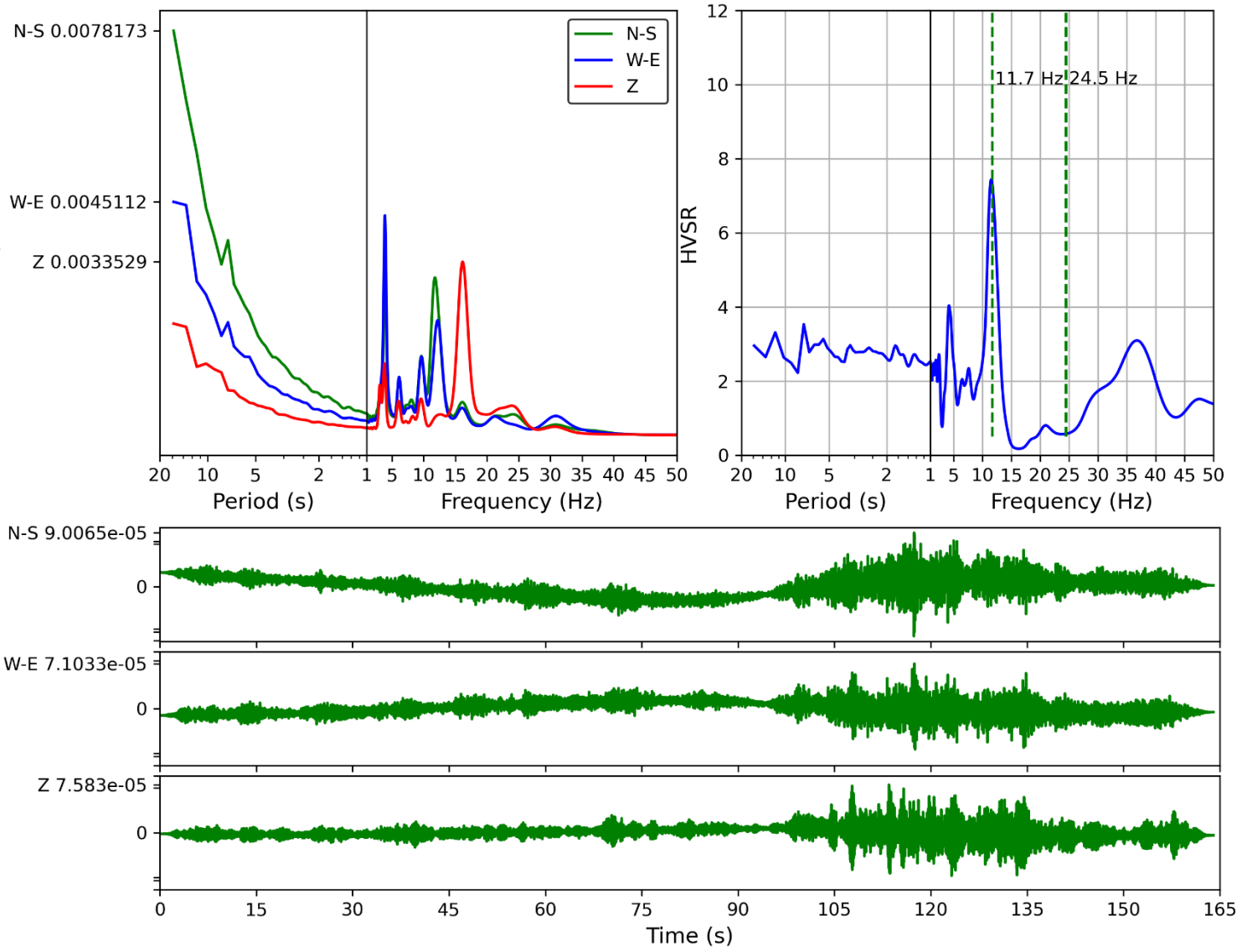

data time span: 2018. 345.061829-2018. 345.062113 (UTC)

Results: Comparison between SP data on lander deck and ground

SP data on ground

Fourier amplitude spectrums

- **smooth** peaks in each component
- several peaks in the frequency range of **12-30** Hz in the horizontal components
- high peak at **28 Hz** in the vertical component

Waveforms

- smaller amplitude in all components
- no obvious tilt in any component

The characteristics of HVSR may be related to the **lander** and **the soil layer**.

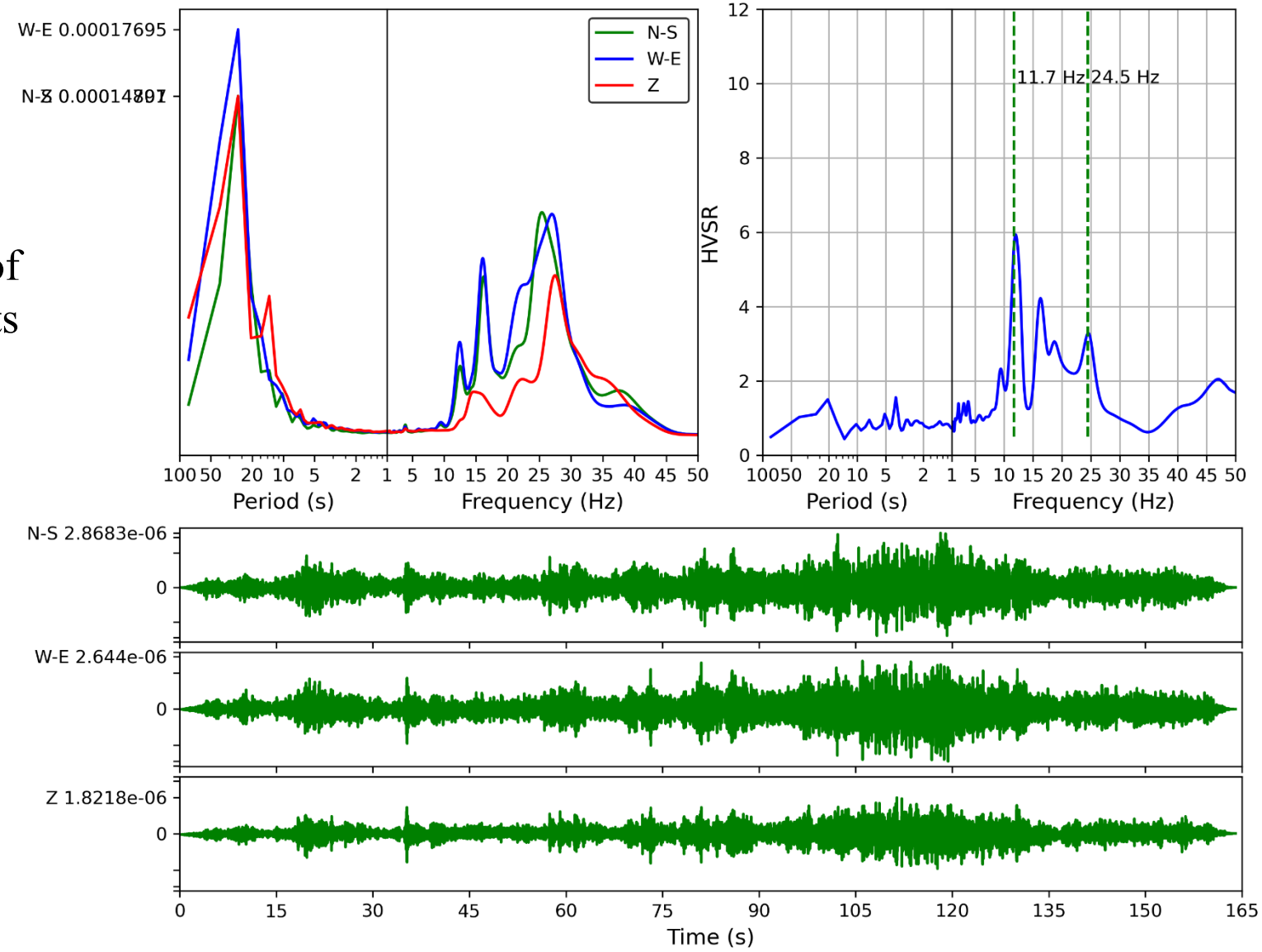

data time span: 2019.041.214438-19.041.214722 (UTC)

Results: Comparison between SP data on lander deck and ground

Damping ratio (DR)

SP data on lander deck
(TS 1-3, data of three time spans in 2018-12)

- DRs generally **below 5%** in all components
- mainly mechanical vibrations

SP data on ground
(TS 1-8, data of eight time spans in 2019-02 and 2019-03)

- DRs generally above 5% in the Z component
- DRs generally below 5% in the horizontal components
- DRs of all components are **below 5%** in most time spans but are above 5% in some time spans.

DRs of SP data on lander deck

	N-S	W-E	Z
TS1	4.69%	2.33%	5.45%
TS2	1.45%	1.22%	2.15%
TS3	3.44%	2.16%	6.00%

DRs of SP data on ground

	N-S	W-E	Z
TS1	2.16%	5.02%	1.95%
TS2	3.40%	2.96%	6.28%
TS3	4.18%	3.93%	4.75%
TS4	4.24%	4.02%	6.57%
TS5	2.27%	2.25%	4.89%
TS6	7.70%	6.27%	6.40%
TS7	4.00%	2.76%	5.12%
TS8	7.00%	5.40%	6.43%

DRs over 5% are marked red.

Results: HVSR over time

HVSR results

time span (SP data on ground)

- UTC: 2019-03-07T22:30:00 to 2019-03-08T23:09:00
- LMST: 99SolT00:00:00 to 99SolT24:39:00

similar HVSR features with previous results

- peak frequency: 11.7 Hz
- mean peak value: 5.8

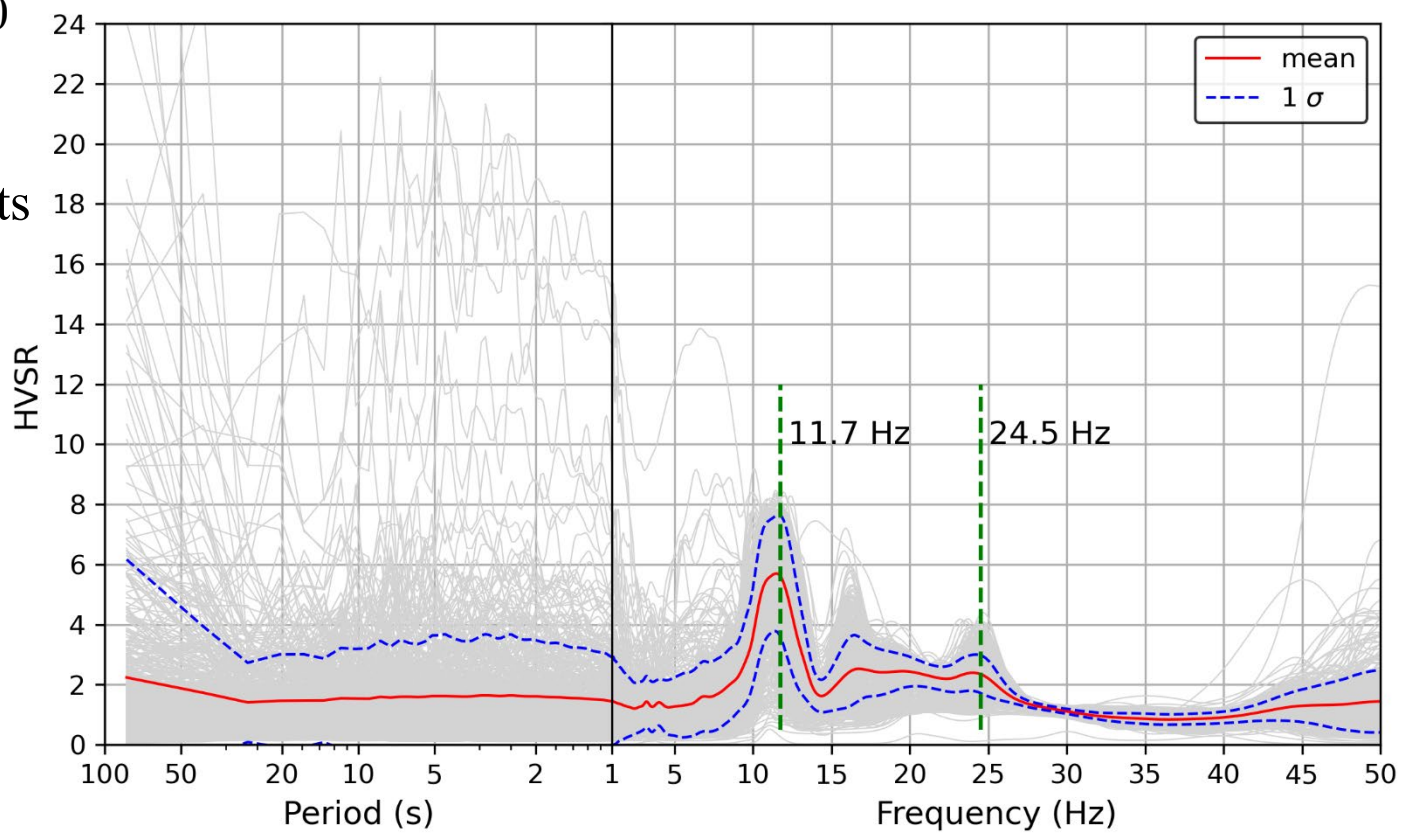

Results: HVSR over time

HVSR results

frequency part above 1.0 Hz

- continuous H/V peak around 11.7 Hz
- high HVSR value in the frequency range of 15-25 Hz

frequency part below 1.0 Hz

- no continuous H/V peak
- High HVSR values may be related to glitches in original data or wind effects (Giardini et al., 2020).

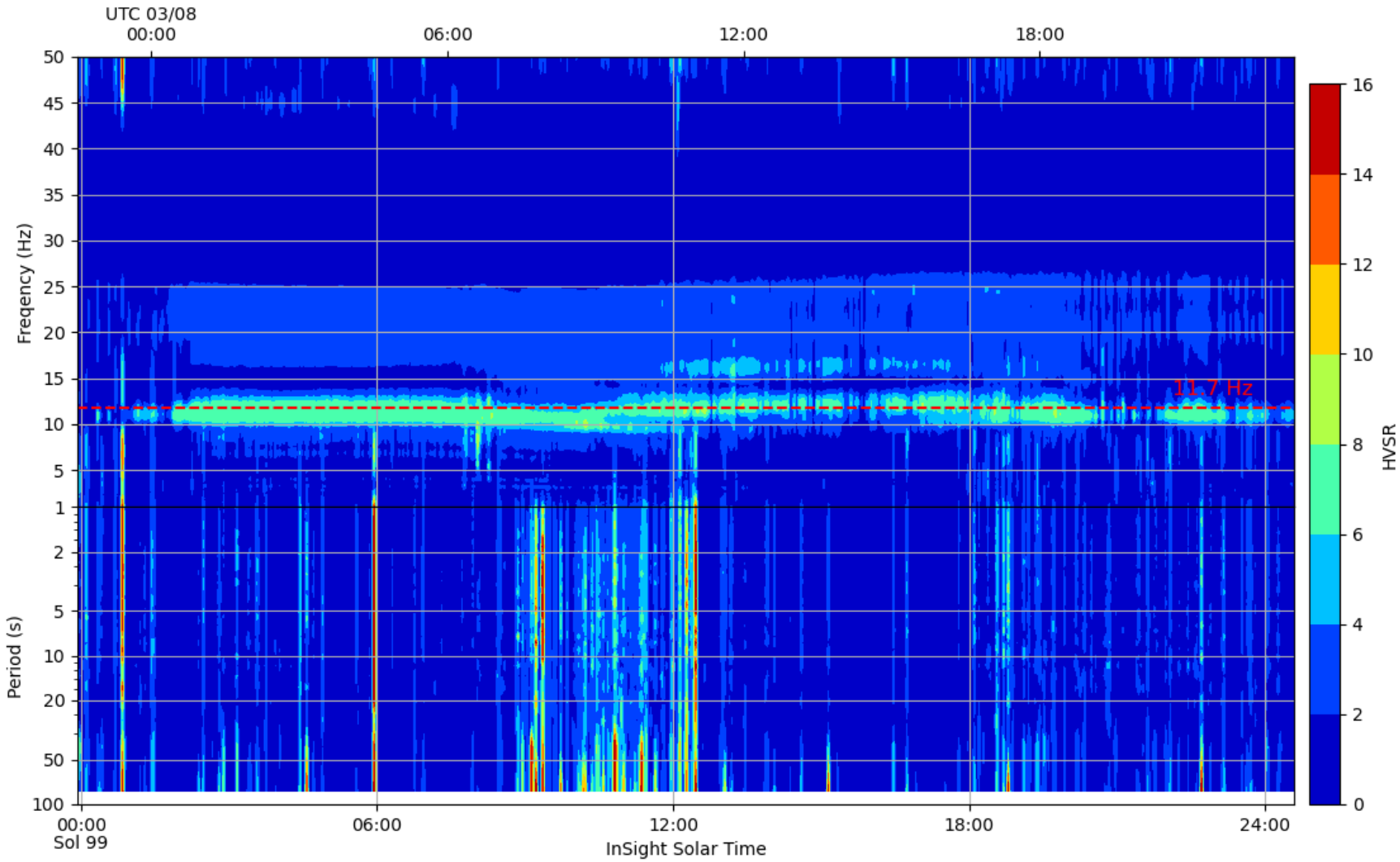

Results: HVSR over time

Meteorological records

- no clear H/V peak for wind speeds below above 2.5 m/s

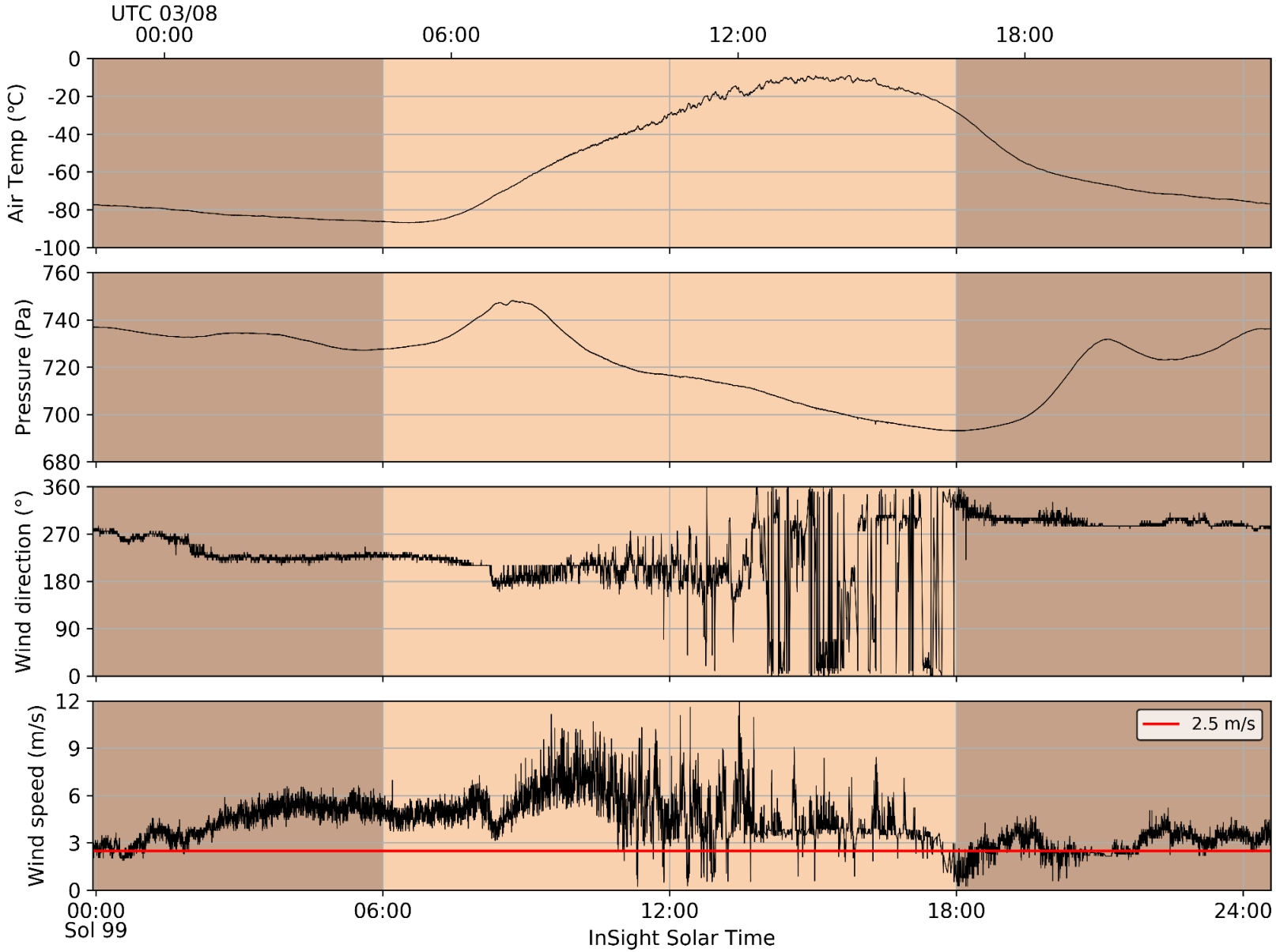

Results: HVSR over time

Damping ratio

- DRs may be related to local wind speed.
- DRs differ in different frequency ranges.

DRs of SP data on ground at 12 Hz (11-13 Hz)

	N-S	W-E	Z
03-07T23:00-24:00	7.49%	5.13%	7.02%
03-08T03:00-04:00	3.79%	3.67%	4.44%
03-08T08:00-09:00	6.47%	5.43%	6.72%
03-08T10:00-11:00	5.85%	5.30%	5.92%
03-08T12:00-13:00	4.99%	4.04%	8.44%
03-08T16:00-17:00	4.55%	4.57%	5.87%
03-08T20:00021:00	5.55%	2.76%	6.44%

DRs of SP data on ground at 24.5 Hz (22-26 Hz)

	N-S	W-E	Z
03-07T23:00-24:00	2.35%	3.01%	3.22%
03-08T08:00-09:00	2.82%	2.83%	2.80%
03-08T10:00-11:00	2.07%	3.35%	4.28%
03-08T20:00021:00	1.59%	2.84%	2.56%

DRs over 5% are marked red.

Summary && Prospect

Summary

- obvious H/V peak of SP data at 11.7 Hz
- relatively high H/V value in the frequency of 12-25 Hz, but no clear H/V peak
- H/V peak value is related to local wind speed.
- SP data on lander deck have low DRs at H/V peak frequency, which indicates mainly mechanical vibrations.
- At 11.7 Hz, DRs of SP data on ground may be related to local wind speed, while at 24.5 Hz, all DRs are below 5%.

Prospect

- more tests on HVSR method and RDM…
- more analyses on DRs of SP data in different time spans…
- explanations of sources of peaks in Fourier amplitude spectrums of each component…
- effects of wind speed and other meteorological conditions on H/V curve…

This study is still in progress and a lot of work remains to be done.
Hopefully I appreciate any comment on this study or any ideas you want to share.
More detailed information about the comment or idea could be sent by email (in the first page) to me if it is convenient for you.
Many thanks for reading!

Supplement

Data citation

- Seismic data are available from http://ds.iris.edu/ds/newsletter/vol21/no1/511/mars-insight-mission-data-from-seis-now-open-to-the-public/
- Meteorological data are available from https://atmos.nmsu.edu/data_and_services/atmospheres_data/INSIGHT/insight.html

References

Alberto Marcellini. GUIDELINES FOR THE IMPLEMENTATION OF THE H/V SPECTRAL RATIO TECHNIQUE ON AMBIENT VIBRATIONS. SAMCO Final Report 2006. Available from www.idpa.cnr.it

Brigitte, Knapmeyer Endrun , et al. "Influence of Body Waves, Instrumentation Resonances, and Prior Assumptions on Rayleigh Wave Ellipticity Inversion for Shallow Structure at the InSight Landing Site." *Space Science Reviews* 214.5(2018):94-136.

Dunand F., Bard P.-Y., Chatelain J.-.L., Guéguen Ph., Vassail T. and Farsi M.N., 2002. Damping and frequency from randomdec method applied to in situ measurements of ambient vibrations: evidence for effective soil structure interaction. Proceedings of the 12th European Conference on Earthquake Engineering, London, 9-13 september 2002.

Ebrahim Haghshenas. Conditions Geotechnique et Alea Sismique Local a Teheran. Sciences de l'ing´ enieur [physics]. Universit´ e Joseph-Fourier - Grenoble I, 2005. Fran¸ cais.

Giardini, D., Lognonné, P., Banerdt, W.B. *et al.* The seismicity of Mars. *Nat. Geosci.* **13,** 205–212 (2020). https://doi.org/10.1038/s41561-020-0539-8

Guillier B., Chatelain J.-L., Bonnefoy-Claudet S., Haghshenas E. (2007) Use of ambient noise: from spectral amplitude variability to H/V stability. J. Earthq. Eng. 11, 925-942, doi:10.1080/13632460701457249

Supplement

References (continued)

Lognonné, P., Banerdt, W.B., Pike, W.T. *et al.* Constraints on the shallow elastic and anelastic structure of Mars from InSight seismic data. *Nat. Geosci.* **13,** 213–220 (2020). https://doi.org/10.1038/s41561-020-0536-y

Mucciarelli, Marco , et al. "The influence of wind on measurements of seismic noise." *Geophysical Journal of the Royal Astronomical Society* 161.2(2005):303-308.

Nakamura, Yosio , et al. "Shallow lunar structure determined from the passive seismic experiment." *Moon* 13.1-3(1975):57-66.

Nakamura, Yosio , and D. L. Anderson . "Martian wind activity detected by a seismometer at Viking Lander 2 site." *Geophysical Research Letters* 6.6(1979):499-502.

Nakamura, Y., 1989. A method for dynamic characteristics estimation of subsurface using microtremor on the ground surface. Q. Rep. Railway Tech. Res. Inst. (RTRI) 30, 25–33.

Tanimoto, T. , S. Ishimaru , and C. Alvizuri . "Seasonality in particle motion of microseisms." *Geophysical Journal International* 1:1.